

## **Deriving long-term time series of sea ice cover from satellite passive-microwave multisensor data sets**

D. J. Cavalieri, C. L. Parkinson, P. Gloersen, J. C. Comiso, and H. J. Zwally

### **Abstract**

We have generated consistent sea ice extent and area data records spanning 18.2 years from passive-microwave radiances obtained with the Nimbus 7 scanning multichannel microwave radiometer and with the Defense Meteorological Satellite Program F8, F11, and F13 special sensor microwave/imagers. The goal in the creation of these data was to produce a long-term, consistent set of sea ice extents and areas that provides the means for reliably determining sea ice variability over the 18.2-year period and also serves as a baseline for future measurements. We describe the method used to match the sea ice extents and areas from these four multichannel sensors and summarize the problems encountered when working with radiances from sensors having different frequencies, different footprint sizes, different visit times, and different calibrations. A major obstacle to adjusting for these differences is the lack of a complete year of overlapping data from sequential sensors. Nonetheless, our procedure reduced ice extent differences during periods of sensor overlap to less than 0.05% and ice area differences to 0.6% or less.

and area, as was done with the F8 SSMI values. A further adjustment to the Antarctic 37V ice type B (see *Gloersen et al.* [1992] for definition of ice types) F11 tie point was also made to reduce the ice area difference. The tie points, the amount of tuning, the ice extent, and area percent differences are all given in Table 3. In this case the amount of tuning needed to reduce the ice extent and area differences between the F8 and F11 values is well within one standard error of estimate (Table 2).

**3.5.3. F11/F13 SSMI overlap.** The 5-month period of overlap for F11 and F13 is much better suited for intersensor corrections than the shorter periods of Nimbus 7 and F8 SSMI overlap and of F8 and F11 SSMI overlap. The linear regression equations obtained from the overlapping data sets and their standard errors of estimates for corresponding channels are given in Table 2. No tuning was needed for the F13 SSMI Arctic open water tie points and only slight tuning was required for the Antarctic 19H open water tie point to reduce differences in ice extent and area. The tie points, the amount of tuning, the ice extent, and area percent differences are all given in Table 3. Presumably, the reason the F13 tie points required so little tuning is that the F11 and F13 sensors differ in ascending node crossing times by less than 45 min (Table 1).

**3.5.4. Results of the correction procedures.** The differences in Arctic ice extents for each pair of sensors during their overlap periods at various steps in the data processing are shown in Figure 4. The first row of plots (Figures 4a–4c) illustrates not only the mismatch in Arctic ice extents, but also the effect of missing SSMI data resulting in sharp drops in ice extent values. The second row (Figures 4d–4f) shows the better agreement after filling data gaps and correcting for land-to-ocean spillover and residual weather effects, and the third row (Figures 4g–4i) shows the results after the algorithm tie point corrections were made. While the initial change in algorithm tie points based on the linear regression relationships discussed in the previous section reduced the differences, the additional minor adjustments to the open water tie points were needed for both the Arctic and Antarctic to reduce the ice extent and area differences to well below 1% (Table 3). The fact that the matching of ice extents and areas was done on a hemispheric basis means that regional differences may be larger [*Stroeve et al.*, 1998]. Examination of Table 3 shows that we obtained better agreement for the ice extent than for the ice area. Also, the differences in ice areas are smaller (better agreement) in general for the winter hemisphere than for the summer hemisphere, and the best agreement is for the F11/F13 pair of SSMI sensors, where the difference in observations times is the smallest. These results are consistent with the fact that diurnal variations in ice concentration (and thus ice area) are larger in summer.

In previous studies, different approaches were used to combine the SMMR and SSMI data sets. *Maslanik et al.* [1996] used an expanded land mask to reduce the difference between SMMR and SSMI ice extents during the overlap period. The SMMR Arctic ice extent in July exceeded the SSMI ice extent by 0.1%, whereas in August the SSMI extent exceeded that of SMMR by 0.3%. In the work by *Björge et al.* [1997], a correction for SMMR – SSMI differences was mentioned, but none for SSMI F8 – F11 differences. *Björge et al.* adjusted the SMMR and SSMI radiances and then adjusted the ice concentration algorithm. Our matching of algorithm coefficients is somewhat comparable to their procedure, but then we additionally match ice extents and areas during the overlap periods.

#### 4. Sea Ice Extent and Area Uncertainties

The calculation of Arctic and Antarctic sea ice concentrations needed to compute sea ice extents and sea ice areas utilizes methods used previously for the SMMR [*Gloersen et al.*, 1992] and SSMI [*Cavaliere et al.*, 1991] data sets. The determination of unbiased long-term trends in a time series of sea ice extent and area depends on the relative accuracy of these parameters throughout the time series and not on their absolute accuracy. Of concern here are sensor drift, errors in matching the different data segments making up the time series, and trends in atmospheric microwave emission. These are all potential sources of error in the determination of trends in the sea ice cover.

For the purpose of examining both sensor drift and potential trends in atmospheric emission over the entire 18.2-year data record, we developed time series of brightness temperatures as well as polarizations (PRs) and spectral gradient ratios (GRs), the two independent variables used in the sea ice concentration algorithm, for ocean areas from 50° latitude (both north and south) to the ice edge for each sensor, following a procedure used previously with the SMMR data [*Gloersen et al.*, 1992]. After the removal of the first and second harmonics of the annual cycle in each of the time series, a linear least squares regression was applied to each of the residual time series, and the change in brightness temperature and in PR and GR were calculated for each sensor. Analyses of these results do not reveal any pattern that would suggest an overall trend either in atmospheric emission or in sensor drift.

The 5-month overlap of the F11 and F13 SSMIs allows the determination of an upper limit of the ice extent and area errors for both the Arctic and Antarctic by calculating the standard deviations of their ice extent and area differences during that time. The estimates are all about 0.3% of the annual mean value and are much less than the estimated long-term trends [*Cavaliere et al.*, 1997a]. It is noteworthy that while the equatorial crossing times of the two spacecraft differ by only 45 min, this estimate may include real fluctuations of the ice covers.

#### 5. Summary

We have described the generation of a seamless time series of sea ice extents and areas spanning 18.2 years based on passive-microwave radiance data obtained from sensors on four satellites. The overall approach taken in the generation of this data set was one of matching geophysical parameters (ice extent and area) by adjusting algorithm tie points rather than changing the input radiances. From analyses of satellite microwave observations, *Zabel and Jezek* [1994] also argued for the calibration and construction of long-term time series at the geophysical product level rather than at the level of measured radiances. While the periods of sensor overlap, which ranged from 2 weeks to 5 months, were less than the desired length of at least 1 year, they served nonetheless to allow the creation of an overall time series with greatly reduced offset errors between the segments from different instruments. Sea ice extent differences were reduced to less than 0.05% and ice area differences to 0.6% or less during the overlap periods.

In the future it is strongly recommended that periods of overlap of at least 1 year in duration be planned when scheduling follow-on launches of operational satellites in order to permit improved intersensor calibrations.

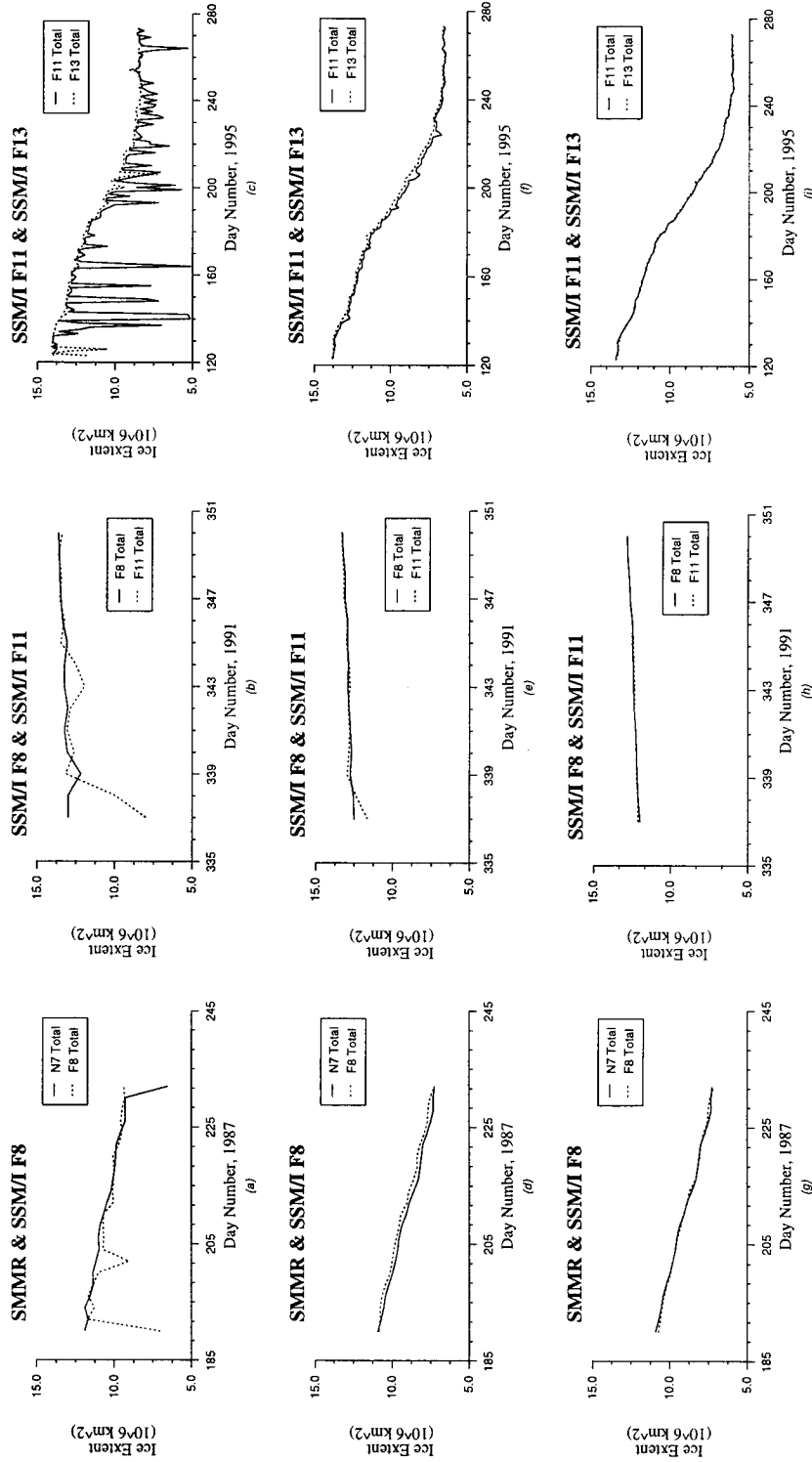


**Figure 4.** Time series of Arctic ice extents during periods of overlap for each pair of sensors (a–c) calculated using uncorrected data, (d–f) calculated after filling data gaps and correcting for land-to-ocean spillover and residual weather effects, and (g–i) calculated after the algorithm tie point corrections were made.

**Acknowledgments.** We gratefully acknowledge the help of S. Fiegles, M. Martino, and J. Saleh from Raytheon STX Corporation with various aspects of this project. We also thank J. Maslanik and J. Stroeve of NSIDC for their help in quality checking the data set. Finally, we thank three anonymous reviewers for their thoughtful comments and very useful suggestions. The SSM/I radiance data were obtained on CD-ROM from NSIDC. This work was supported by Polar Programs at NASA Headquarters.

## References

- Bjørge, E., O. M. Johannessen, and M. W. Miles, Analysis of merged SMMR-SSM/I time series of Arctic and Antarctic sea ice parameters 1978–1995, *Geophys. Res. Lett.*, **24**, 413–416, 1997.
- Cavalieri, D. J., J. Crawford, M. R. Drinkwater, D. Eppler, L. D. Farmer, R. R. Jentz, and C. C. Wackerman, Aircraft active and passive microwave validation of sea ice concentration from the DMSP SSM/I, *J. Geophys. Res.*, **96**, 21,989–22,008, 1991.
- Cavalieri, D. J., K. St. Germain, and C. T. Swift, Reduction of weather effects in the calculation of sea ice concentration with the DMSP SSM/I, *J. Glaciol.*, **41**, 455–464, 1995.
- Cavalieri, D. J., P. Gloersen, C. L. Parkinson, J. C. Comiso, and H. J. Zwally, Observed hemispheric asymmetry in global sea ice changes, *Science*, **272**, 1104–1106, 1997a.
- Cavalieri, D. J., C. L. Parkinson, P. Gloersen, and H. J. Zwally, Arctic and Antarctic sea ice concentrations from multichannel passive-microwave satellite data sets: October 1978–September 1995: User's guide, *NASA Tech. Memo. 104647*, 17 pp., NASA, Washington, D. C., 1997b.
- Colton, M. C., and G. A. Poe, Intersensor calibration of DMSP SSM/I's: F-8 to F-14, 1987–1997, *IEEE Trans. Geosci. Remote Sens.*, **37**, 418–439, 1999.
- Fiegles, S., and P. Gloersen, Arctic sea ice: 1978–1996, ReadMe file on CD-ROM, NASA, Washington, D. C., 1998.
- Fischer, H., and C. Oelke, Sea ice concentration in response to weather systems in the Weddell Sea: Comparison between SSM/I data and model simulations, paper presented at the 1997 International Geoscience and Remote Sensing Symposium, Inst. of Electr. and Electron. Eng., Singapore, Aug. 3–8, 1997.
- Gloersen, P., and F. T. Barath, A scanning multichannel microwave radiometer for Nimbus-G and SeaSat-A, *IEEE J. Oceanic Eng., OE-2*, 172–178, 1977.
- Gloersen, P., and D. J. Cavalieri, Reduction of weather effects in the calculation of sea ice concentration from microwave radiances, *J. Geophys. Res.*, **91**, 3913–3919, 1986.
- Gloersen, P., W. J. Campbell, D. J. Cavalieri, J. C. Comiso, C. L. Parkinson, and H. J. Zwally, *Arctic and Antarctic Sea Ice, 1978–1987: Satellite Passive-Microwave Observations and Analysis*, *Spec. Publ. 511*, 290 pp., NASA, Washington, D. C., 1992.
- Gloersen, P., C. L. Parkinson, D. J. Cavalieri, J. C. Comiso, and H. J. Zwally, Spatial distribution of trends and seasonality in the hemispheric sea ice covers: 1978–1996, *J. Geophys. Res.*, this issue.
- Johannessen, O. M., M. W. Miles, and E. Bjørge, The Arctic's shrinking sea ice, *Nature*, **376**, 126–127, 1995.
- Levitus, S., and T. P. Boyer, *World Ocean Atlas 1994*, vol. 4, *Temperature*, NOAA Natl. Oceanogr. Data Cent., Ocean Clim. Lab., U.S. Dep. of Commerce, Washington, D. C., 1994.
- Martino, M., D. J. Cavalieri, P. Gloersen, and H. J. Zwally, An improved land mask for the SSM/I grid, *NASA Tech. Memo. 104625*, 9 pp., 1995.
- Maslanik, J. A., Effects of weather on the retrieval of sea ice concentration and ice type from passive microwave data, *Int. J. Remote Sens.*, **1391**, 37–54, 1992.
- Maslanik, J. A., M. C. Serreze, and R. G. Barry, Recent decreases in Arctic summer ice cover and linkages to atmospheric circulation anomalies, *Geophys. Res. Lett.*, **23**, 1677–1680, 1996.
- National Snow and Ice Data Center (NSIDC), DMSP SSM/I brightness temperatures and sea ice concentration grids for the polar regions, on CD-ROM User's Guide, *Natl. Snow Ice Data Cent. Spec. Rep. 1*, Cooperative Inst. for Res. in Environ. Sci., Univ. of Colo., Boulder, Jan. 1992.
- Oelke, C., Atmospheric signatures in sea-ice concentration estimates from passive microwaves: Modelled and observed, *Int. J. Remote Sens.*, **18**, 1113–1136, 1997.
- Parkinson, C. L., J. Comiso, H. J. Zwally, D. J. Cavalieri, P. Gloersen, and W. J. Campbell, *Arctic Sea Ice, 1973–1976: Satellite Passive-Microwave Observations*, *Spec. Publ. 489*, 296 pp., NASA, Washington, D. C., 1987.
- Parkinson, C. L., D. J. Cavalieri, P. Gloersen, H. J. Zwally, and J. C. Comiso, Arctic sea ice extents, areas, and trends, 1978–1996, *J. Geophys. Res.*, this issue.
- Project for Estimation of Long-Term Variability of Ice Concentration (PELICON), Final report under EC contract EV5V-CT93-0268 (DG 12 DTEE), 188 pp., Eur. Comm., Brussels, July 1996.
- Stroeve, J., J. Maslanik, and L. Xiaoming, An intercomparison of DMSP F-11- and F13-derived sea ice products, *Remote Sens. Environ.*, **64**, 132–152, 1998.
- Zabel, I. H. H., and K. C. Jezek, Consistency in long-term observations of oceans and ice from space, *J. Geophys. Res.*, **99**, 10,109–10,120, 1994.

---

D. J. Cavalieri, J. C. Comiso, P. Gloersen, C. L. Parkinson, and H. J. Zwally, Laboratory for Hydrospheric Processes, NASA Goddard Space Flight Center, Greenbelt, MD 20771. (e-mail: don@cavalieri.gsfc.nasa.gov)

(Received June 15, 1998; revised February 22, 1999; accepted March 17, 1999.)